EFFECT OF DIVALENT CATIONS ON POTASSIUM CONDUCTANCE OF SQUID AXONS: DETERMINATION OF SURFACE CHARGE

DANIEL L. GILBERT *and* GERALD EHRENSTEIN

From the Laboratory of Biophysics, National Institute of Neurological Diseases and Stroke, National Institutes of Health, Bethesda, Maryland 20014 and the Marine Biological Laboratory, Woods Hole, Massachusetts 02543

ABSTRACT Potassium conductance-voltage curves have been determined for a squid axon in high external potassium solution for a wide range of divalent cation concentrations. A decrease in divalent ion concentration shifts the conductance-voltage curve along the voltage axis in the direction of more hyperpolarized voltages by as much as 9 mv for an *e*-fold change in concentration. When the divalent ion concentration is less than about 5 mM, a further decrease does not cause a significant shift of the conductance-voltage curve. These results can be explained by assuming that on the outer surface of the membrane there is a negative fixed charge which can bind calcium ions, and that the axon is sensitive to the resulting double-layer potential. From our data, the best value for charge density was found to be one electronic charge per 120 square angstroms, and a lower limit to be one electronic charge per 280 square angstroms.

INTRODUCTION

Frankenhaeuser and Hodgkin (1957) presented evidence that the potassium conductance vs. voltage curve is shifted along the voltage axis as the external calcium concentration is varied. They also described an explanation suggested by A. F. Huxley that calcium ions may be adsorbed at the outer edge of the membrane and thereby create an additional electric field inside the membrane without changing the over-all potential difference between inside and outside. We consider a more specific model of this type. We assume that there is a negative fixed charge at the outer surface of the membrane giving rise to a double-layer potential, and that calcium can bind to this fixed charge, thus partially neutralizing it. This model predicts the observed direction of the shift of the potassium conductance curve along the voltage axis. It also predicts that when the calcium concentration is sufficiently low, a further decrease would cause only a slight further shift along the axis. This is because in low calcium solution very little calcium is bound to the fixed charge and so a further decrease in the amount of calcium bound has little effect.

In order to test this prediction, we have measured potassium conductance-voltage curves over a large range of calcium concentrations in high potassium solutions. High potassium concentration in the external solution enables us to use very low calcium concentrations without the problem of repetitive firing. Also, we avoid the difficulty, pointed out by Frankenhaeuser and Hodgkin, that for axons immersed in an artificial sea water and voltage clamped near the resting potential, other ions beside potassium contribute substantially to the steady-state current.

A preliminary report of some of the results has previously been given (Gilbert and Ehrenstein, 1965).

METHODS

Squid (*Loligo pealei*) axons were voltage clamped at 10°C in a manner previously described (Ehrenstein and Gilbert, 1966), unless otherwise indicated. Increasing depolarizing pulses were applied before increasing hyperpolarizing pulses in order to obtain reproducible results (Ehrenstein and Gilbert, 1966). By this procedure the effects of long time constants on the potassium current were minimized. A liquid junction potential of −4 mv was assumed (Cole and Moore, 1960). The relative osmolarity was measured by the vapor pressure method at 37°C with reference to the artificial seawater (ASW) composed of 10 mM potassium, 430 mM sodium, 10 mM calcium, 50 mM magnesium, 560 mM chloride, and buffered with 0.5 mM tris(hydroxymethyl)aminomethane (Tris) to a pH of 7.8 ± 0.1. Unless otherwise stated all solutions contained 0.5 mM Tris, were at a pH of 7.8 ± 0.1, and chloride ion was the only anion. The other constituents used and the corresponding values of relative osmolarity for the high potassium solutions are given in Table I.

In one set of experiments, the effect of a chelating agent, ethylene glycol *bis* (β-aminoethylether)-N,N′-tetraacetic acid (EGTA), was investigated. The log of the binding constant of EGTA for calcium is 10.7 (Schmid and Reilley, 1957). For this set of experiments the solutions were buffered with 5 mM Tris instead of 0.5 mM Tris; and the control solution

TABLE I

CATIONIC COMPOSITION AND RELATIVE OSMOLARITY OF HIGH POTASSIUM SOLUTIONS

Solution	Potassium	Calcium	Magnesium	Relative osmolarity (Artificial seawater = 1.000)
	mM	mM	mM	
A	500	0	0	0.948
B	500	2	0	0.913
C	500	0	10	0.950
D	440	0	50	0.949
E	440	10	50	0.988
F	440	40	50	1.069
G	440	160	50	1.438
H	215	160	50	0.971

contained 500 mM potassium, whereas the experimental solution contained 480 mM potassium plus 10 mM EGTA. Also, the artificial seawater was buffered with 5 mM Tris.

Conductance curves were obtained by dividing the steady-state currents (currents at 40 msec) by the difference between holding potential and the potassium equilibrium potential. The resulting conductances were then normalized by making the maximum conductance for each curve equal to one.

For values of resting membrane potentials within about 30 mv from zero, the potassium equilibrium potential approximates the resting membrane potential (Curtis and Cole, 1942). Therefore, for all solutions used, with the exception of the artificial seawater solution, it was assumed that the potassium equilibrium potential was equal to the resting membrane potential. For the artificial seawater solution, the potassium equilibrium potential was calculated according to the Nernst potential assuming an internal potassium concentration of 400 mM (Hodgkin, 1958).

For the part of the conductance curve in which the slope is positive, the negative potential ($V_{1/2}$) at which the conductance is the average between the maximum and minimum was measured, and was used as a convenient measure of potential effects.

In a few experiments, the currents were divided into a linear and a nonlinear component (Lecar et al., 1967), and the conductances of these components were determined.

RESULTS

In Fig. 1, current-voltage curves are shown for solutions in which the potassium concentration is high, and the divalent cation concentration is varied. Curve II of Fig. 1 has two negative resistance regions, one for positive and one for negative values of voltage. The one for negative values of voltage is more pronounced, and corresponds to the negative resistance region of curves I and III. The effect of decreasing the divalent cation concentration is to shift this negative resistance region to the left and also to increase the magnitude of the inward current.

In order to separate these two effects and to demonstrate the voltage shift more clearly, normalized conductance curves were plotted (Fig. 2) for the data shown in Fig. 1. Included in this graph for comparison is also a steady-state conductance curve for an axon immersed in artificial seawater. All the curves show the same general shape; the effect of decreasing the divalent cation concentration is to shift the conductance and the curves to the left. The linear and nonlinear components of current were separated. Table II shows that the $V_{1/2}$ value for the nonlinear component of the conductance is practically the same as the $V_{1/2}$ value for the total conductance. Since potassium is the principal cation carrying current, both the linear and nonlinear components of conductance should be affected to the same extent. In Table III and in the calculations to follow, $V_{1/2}$ for the total conductance curves were used.

Table III gives results of 20 experiments in which the divalent ion concentration was varied. Generally, the effect of decreasing the divalent ion concentration was to make $V_{1/2}$ more negative. However, for low values of divalent cation concentration, very little effect on $V_{1/2}$ was observed. Decreasing the divalent ion concentration also increased the maximum steady-state conductance and had almost no effect on the resting membrane potential.

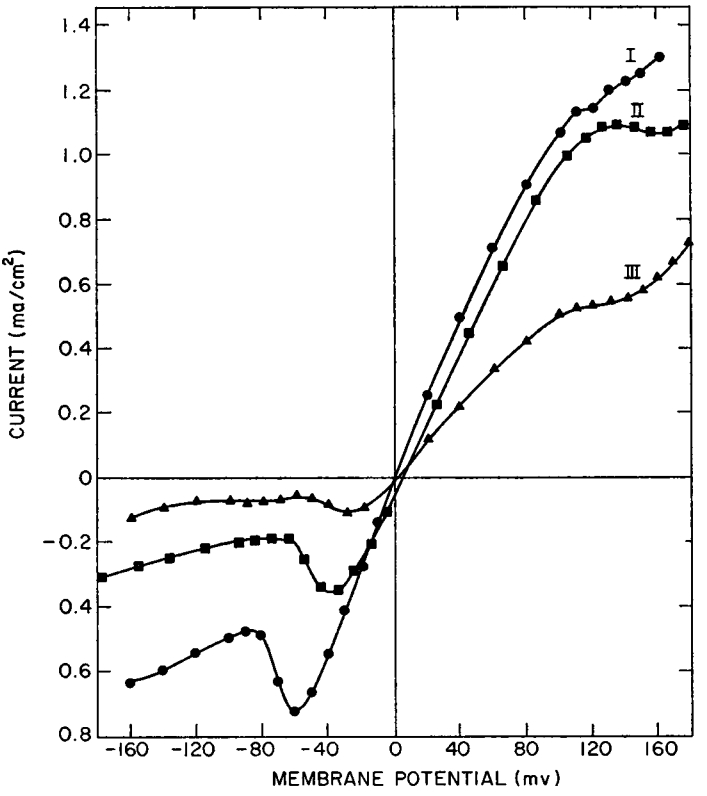

FIGURE 1 Steady-state current (positive outward) vs. membrane potential (outside zero) in high external potassium solutions. For each run, axon clamped at resting potential (R.P.) I ● 0 mM Ca^{++}, 0 mM Mg^{++}, 500 mM K^+, 0 mv R.P. II ■ 10 mM Ca^{++}, 50 mM Mg^{++}, 440 mM K^+, 6 mv R.P. III ▲ 160 mM Ca^{++}, 50 mM Mg^{++}, 440 mM K^+ 1 mv R.P.

The effect of the high calcium solution (Fig. 2) could be due to the fact that the solution was hyperosmotic, as was necessary to keep the potassium concentration relatively constant. Therefore, the potassium concentration was decreased to make the solution isosmotic. Fig. 3 compares the conductance curves for the hyperosmotic and osmotic high-calcium solutions and shows that there is no hyperosmotic effect on the steady-state conductance.

Manufacturer's analysis of the potassium chloride showed that some calcium was present as an impurity. For the 0.5 M potassium chloride used in our nominal divalent cation-free solution, this amounts to 0.01 mM calcium. Leakage of calcium from the axon and Schwann cell could increase the calcium, perhaps to 0.1 mM. In an effort to reduce the calcium in the external medium, a calcium-chelating agent (EGTA) was added to a divalent cation-free solution. As shown in Fig. 4, the steady-state conductance of the 10 mM EGTA divalent cation-free solution was not changed from the steady-state conductance of the divalent cation-free solution.

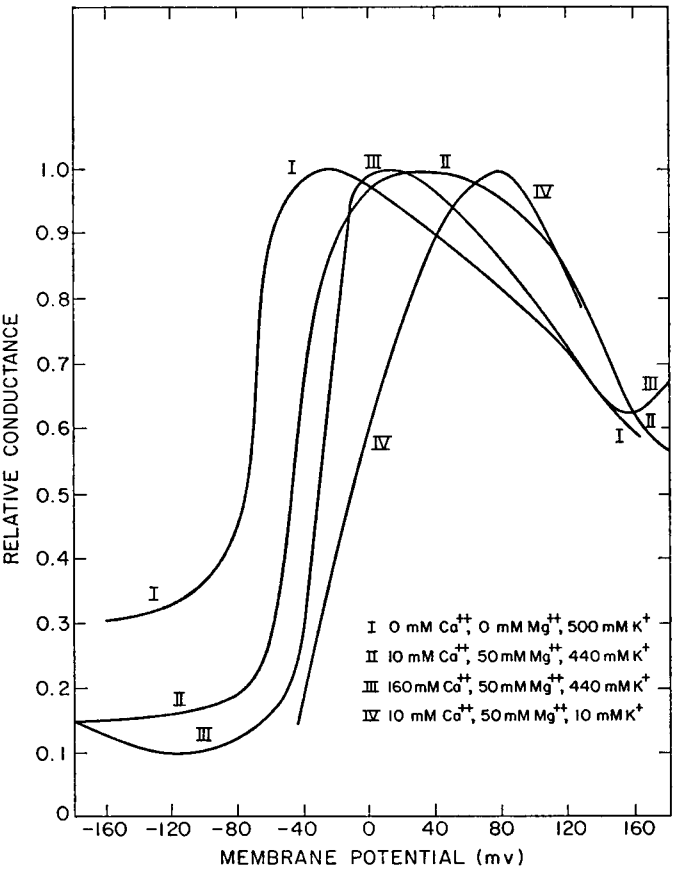

FIGURE 2 Steady-state conductance vs. membrane potential. Curves I, II, and III correspond to curves I, II, and III in Fig. 1. Curve IV is for an axon immersed in seawater.

TABLE II

ANALYSIS OF TYPICAL EXPERIMENTS INTO LINEAR AND NONLINEAR CONDUCTANCE COMPONENTS

Calcium	Magnesium	Linear conductance	Maximum nonlinear conductance	$V_{1/2N.L.}$	$V_{1/2total}$
mM	*mM*	*mmho/cm²*	*mmho/cm²*		
0	0	4.20	9.44	−70	−72
10	50	1.72	9.50	−46	−44
160	50	0.740	5.50	−31	−31

$V_{1/2N.L.}$ is the membrane potential at which the conductance is one-half the maximum conductance for the nonlinear component.

TABLE III

EFFECT OF DIVALENT ION CONCENTRATION ON NERVE PROPERTIES

Calcium	Magnesium	No. of exp	$V_{1/2}$	Maximum conductance	Resting potential
mM	*mM*		*mv*	*mmho/cm²*	*mv*
0	0	4	−67 ± 2.4	15.9 ± 2.5	1.5 ± 1.3
2	0	3	−61.3 ± 6.1	13.0 ± 1.6	1.3 ± 2.0
0	10	2	−70 ± 4	11.6 ± 0.8	5 ± 1
0	50	1	−63	15.1	3
10	50	5	−43.6 ± 3.4	7.9 ± 1.4	1.2 ± 1.5
40	50	1	−48	13.7	2
160	50	4*	−29 ± 1.1	6.5 ± 0.5	—

* Two experiments contained 215 mM potassium and two experiments contained 440 mM potassium. Since no difference was observed, they were grouped together.

$V_{1/2}$ is the membrane potential at which the conductance is one-half the maximum conductance. All the nerves were immersed in either 500 or 440 mM potassium, unless otherwise indicated.

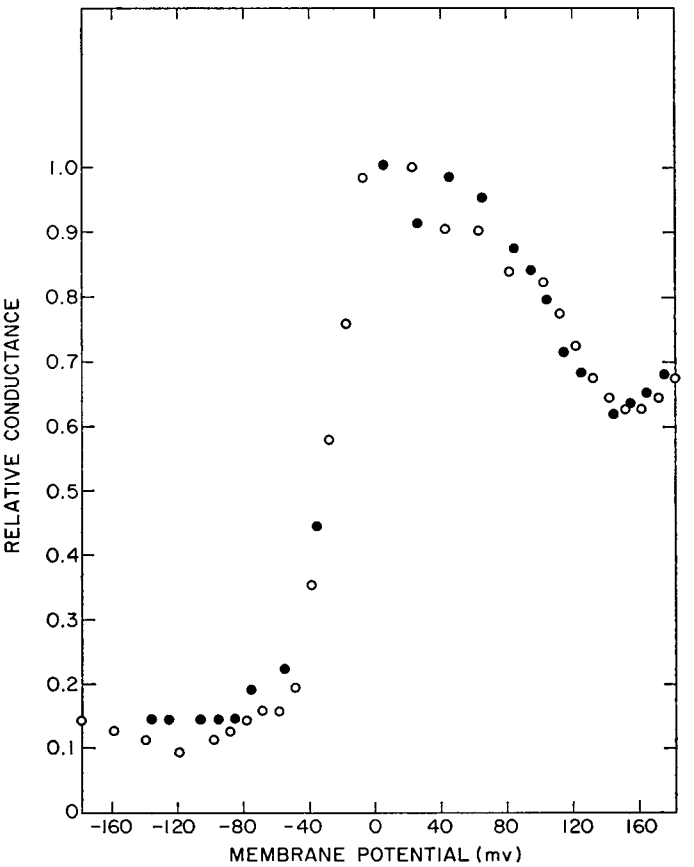

FIGURE 3 Steady-state conductance in high calcium solutions. ○ 160 mM Ca^{++}, 50 mM Mg^{++}, 440 mM K^+; maximum conductance = 6.2 mmho/cm²; resting potential = 1 mv. ● 160 mM Ca^{++}, 50 mM Mg^{++}, 215 mM K^+; maximum conductance = 6.3 mmho/cm²; resting potential = −17 mv.

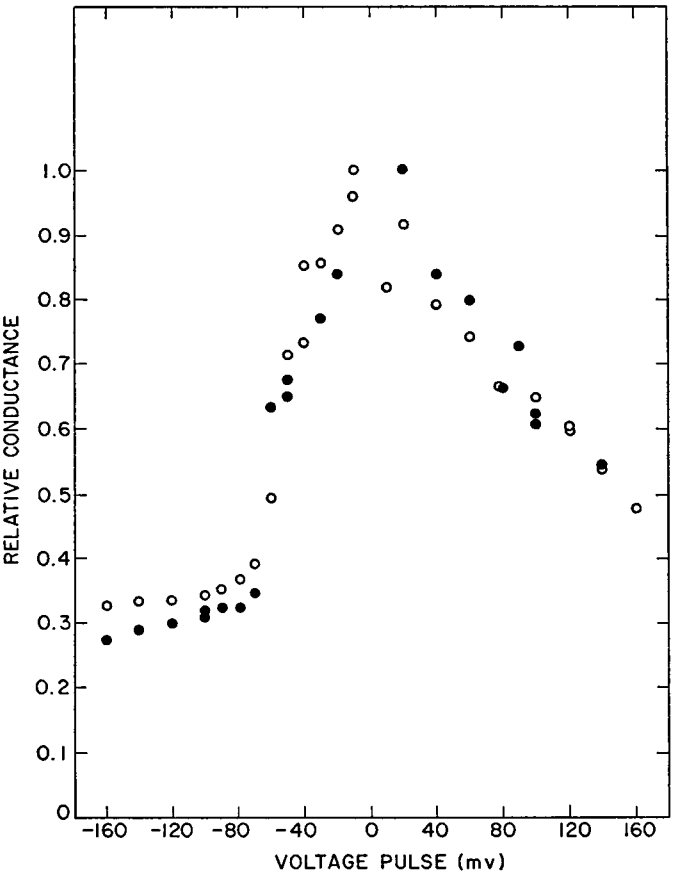

FIGURE 4 Steady-state conductance in divalent cation-free solutions. ○ 500 mM K^+. ● 480 mM K^+, 10 mM EGTA.

DISCUSSION

Relative Effectiveness of Calcium and Magnesium

In order to plot all the data shown in Table II, it is necessary to make some assumption as to the relative effectiveness of calcium and magnesium in shifting the conductance curve. In Fig. 5, the shifts of conductance shown in Table III are plotted as a function of divalent ion concentrations for three assumptions of the relative effectiveness of calcium and magnesium.

It has been shown (Frankenhaeuser and Hodgkin, 1957) that magnesium is about half as effective as calcium in shifting the conductance curve in seawater, and it is likely that the same ratio applies to the high potassium solutions we have used. This is one of the assumptions used in Fig. 5. The other assumptions were extreme cases:

(*a*) magnesium is just as effective as calcium.

(*b*) magnesium is completely ineffective.

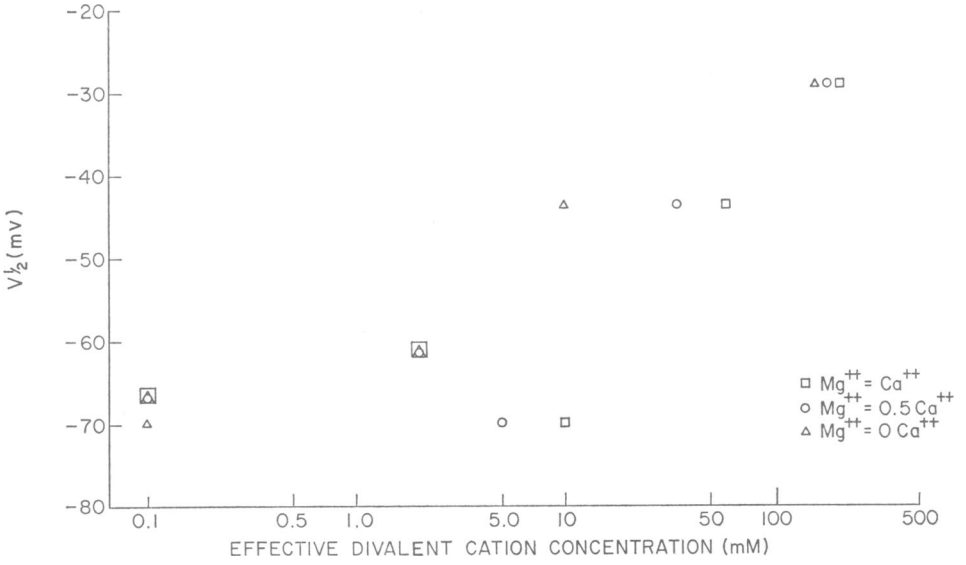

FIGURE 5 Effect of divalent cation concentration on shift of steady-state conductance curves. □ Assuming Mg and Ca are equally effective. ○ Assuming Mg is half as effective as Ca. △ Assuming Mg is completely ineffective.

Negative Fixed Charge Model

In this paper, we invoke a negative fixed charge model to explain the voltage shift of the conductance curve caused by varying the divalent cation concentration. We do not have an adequate explanation for the magnitude change. Perhaps, it is due to some channels becoming completely nonfunctional.

We assume a negative fixed charge uniformly distributed over the outer surface of the axon membrane (Tasaki et al. 1961), at least in the vicinity of the potassium channel. A negative fixed charge on the inner surface of the membrane has been invoked by Chandler et al. (1965) to explain shifts of sodium conductance parameters along the voltage axis when the ionic strength is varied. We further assume that calcium ions from the external solution can bind to the negative fixed charges, thus tending to neutralize them. There is evidence that calcium might bind to the biological membrane (Manery, 1966). The negative fixed charge that is not neutralized by calcium gives rise to a diffuse double layer since the cations in the external solution are preferentially attracted toward the membrane surface while the anions are repelled. This causes the outer surface of the membrane to be more negative than the bulk of the external solution. If we adopt the usual convention of designating the membrane voltage as the intracellular electrical potential minus the extracellular electrical potential, then the effect of the negative fixed charge on the external surface is to make the membrane potential more positive. Thus, if calcium concentration is

decreased, the negative fixed charge is increased and the membrane voltage is made more positive. Therefore, less positive voltage-clamp pulses are required to obtain a given conductance, and decreased calcium concentration should shift the conductance curve to the left, as it does in Fig. 2. Furthermore, the shift should be a simple translation along the voltage axis, which is in rough agreement with Fig. 2. When calcium concentration is sufficiently reduced so that very little is bound to the negative fixed charges, further reduction will not change the potential significantly, and the conductance curve will not be shifted much more. Similarly, the conductance shift should saturate for high calcium concentration. Fig. 5 clearly demonstrates the low calcium saturation, but the high calcium saturation cannot be seen. We assume this is because of the experimental limitation on high calcium concentration.

In these experiments, we are essentially titrating the negative fixed charge with divalent cations. The difference between the asymptotic potentials for very high and very low divalent cation concentrations is a measure of the titratable surface fixed charge density. The total fixed charge density may be greater because some negative fixed charge is not titratable or because univalent potassium cations bind to some sites. In fact, there is evidence for the latter (Goodford, 1966; Goldman, 1968; Ehrenstein and Gilbert, 1968).

Since we have only observed one asymptote, we cannot directly determine the fixed charge density. But we can make use of the shape of the curve relating voltage shift to divalent cation concentration to estimate the missing asymptote, and thus the fixed charge density. Also, without resorting to curve fitting, we can set a lower limit for the difference between asymptotes, and thus set a lower limit for the fixed charge density.

Derivation of Relation Between Divalent Cation Concentration and Voltage Shift

The potential difference across the double-layer increases with increasing charge density of the membrane phase, but decreases with increasing ionic concentration in the solution. The reason is that the potential difference depends roughly on the product of the double-layer charge magnitude and the average separation between positive and negative charges. As the ionic concentration in the solution is increased, there are more counterions close to the surface, and the average charge separation is decreased.

According to the kinetic theory of the diffuse double-layer (Grahame, 1947), the expression relating the double-layer potential, the surface fixed charge density and the ionic concentrations in the solution is:

$$\sigma = \frac{1}{G}\left[\sum_{i=1}^{n} C_i \left(\exp \frac{-Z_i FV}{RT} - 1\right)\right]^{1/2} \qquad (1)$$

where σ = negative fixed charge density
G = constant at a given temperature
n = number of ionic species
C_i = concentration in the external solution of ionic species i
Z_i = valence of ionic species i
F = Faraday = 96,500 coul/mole
V = potential difference across the double-layer
R = gas constant = 8.314 joule/°K mole
T = temperature of the axon = 283° K

The parameter G is a function of the dielectric constant and temperature:

$$G = \left(\frac{F}{N}\right)\left(\frac{2\pi}{RTDD_0}\right)^{1/2} \tag{2}$$

where N = Avogadro's number = $6.02 \cdot 10^{23}$ electron/mole
D = dielectric constant of water = 84.11 at T
D_0 = permittivity of free space = (4π) $(8.85 \cdot 10^{-12}$ coul^2/newt m$^2)$

When C is expressed in moles/liter and σ is expressed in electronic charge/square A, then $G = 270\left(\frac{\text{A}^2}{\text{electronic charge}}\right)$ (mole/liter)$^{1/2}$. The negative fixed charge density can also be expressed as follows:

$$\sigma = \frac{1}{A} = \frac{1}{d^2} \tag{3}$$

where A = average area per electronic charge
d = average spacing between charges

The Donnan or Boltzman factor can be used to determine C_{m_i}, the concentration of ionic species i at the external membrane surface, as follows:

$$C_{m_i} = C_i e^{-HZ_iV} \tag{4}$$

where

$$H = \frac{F}{RT}. \tag{5}$$

The value of $H = 0.041$ mv^{-1}. V is the potential at the external membrane surface minus the potential in the external solution. This potential difference is, therefore, negative for the negatively charged membrane. It is related to our measured $V_{1/2}$ by:

$$V = V_{1/2} - B \tag{6}$$

where B and $V_{1/2}$ are in mv and B is an unknown constant.

Some important approximations have been made in the derivation of equation 1.

It is assumed that the dielectric constant in the double layer is constant and is equal to the dielectric constant of the solvent in the bulk solution. The negative fixed charge sites are also assumed to be uniformly distributed on the membrane surface.

In the derivation of equation 1 the electric field in the membrane is neglected. This electric field appears to be quite small compared to the electric field in the external solution in all our experiments, since we always used high ionic concentrations, i.e., at least 0.5 M (Chandler et al., 1965).

We assume that the negatively charged sites on the membrane can be neutralized by divalent cations. The equilibrium constant for such a neutralization is:

$$k = \frac{MS}{M_m S} \tag{7}$$

where k = equilibrium constant
M_m = effective divalent cation concentration at the membrane
S = free negatively charged site concentration
MS = neutralized site concentration

The relation between M_m, the effective divalent cation concentration at the membrane, and M, the effective divalent cation concentration in the external solution is given by equation 4 where the valence is equal to two. The maximum number of sites is:

$$S_t = S + MS \tag{8}$$

where S_t = maximum number of sites.

Combining equations 7 and 8 results in:

$$\frac{S}{S_t} = \frac{1}{kM_m + 1}. \tag{9}$$

Since the negative fixed charge is equal to $-ZN$ times the concentration of free sites,

$$\frac{\sigma}{\sigma_t} = \frac{-ZNS}{-ZNS_t} = \frac{1}{kM_m + 1} \tag{10}$$

where σ_t = maximum surface charge. When $\sigma = \sigma_t$, then $A = A_t$, $d = d_t$, $V = V_t$, and $V_{1/2} = V_{1/2_t}$.

Since the negatively fixed charge sites become neutralized by the divalent cations, it is implicit in our derivation of equation 10 that the negatively fixed charge sites have an effective valence of minus two. We have also ignored any nonspecific adsorption.

Combining equations 1, 3, 5, 6, and 10 results in:

$$d_t^2[kMe^{2H(B-V_{1/2})} + 1] = \frac{G}{\left\{\sum_{i=1}^{n} C_i[e^{Z_iH(B-V_{1/2})} - 1]\right\}^{1/2}}. \quad (11)$$

Equation 11 gives the relation between M and $V_{1/2}$. In our experiments, the ionic constituents were K^+, Cl^-, Ca^{++}, and Mg^{++}, so that n equals four.

Determination of Surface Fixed Charge Density

There are three unknowns (d_t, k, and B) in equation 11, and we can determine them by fitting this equation to our 20 experimental points. This is shown in Fig. 6, where we have assumed that the effective divalent cation concentration is the sum of the calcium concentration plus one-half the magnesium concentration (cf. Fig. 5). The parameters used for the curves in Fig. 6 are: d_t = 10 A, B = 2 mv, and k = 0.0001 mM^{-1}.

The lower solid curve and the dashed curve were calculated for a potassium concentration of 0.50 M and a magnesium concentration of zero, and should correspond to our data up to an effective divalent cation concentration of 25 mM. The upper

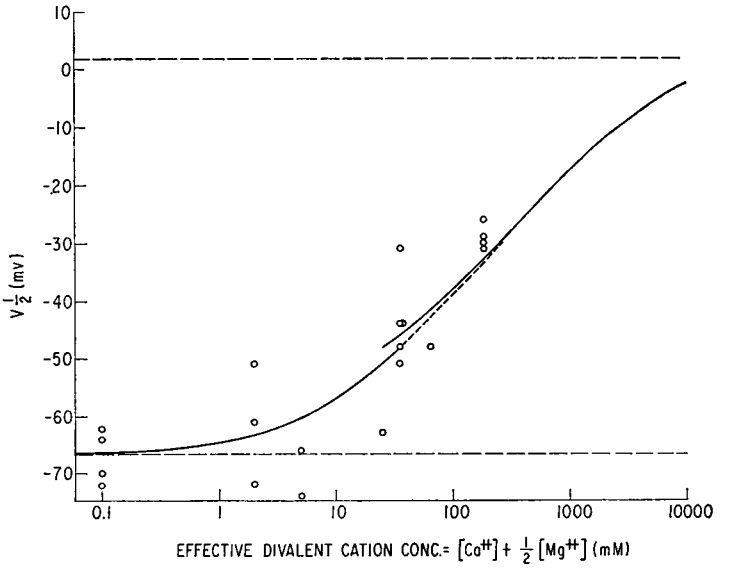

FIGURE 6 Theoretical fit of experimental voltage shifts for various divalent cation concentrations. The curves were calculated from equation 11. The lower solid curve was obtained for potassium equal to 0.5 M and magnesium equal to zero. It is valid for our data up to an effective divalent cation concentration of 25 mM. The upper solid curve was obtained for potassium equal to 0.44 M and magnesium equal to 0.05 M. It is valid for effective divalent cation concentration of 25 mM or more.

solid curve was calculated for a potassium concentration of 0.44 M and a magnesium concentration of 0.05 M, and should correspond to our data for greater effective divalent cation concentrations. The difference between the two curves is quite small, and is negligible at high divalent cation concentrations.

In Fig. 6, two of the points for M = 185 mM were obtained from experiments where the potassium concentration was only 215 mM. According to equation 11, however, this would change the ordinate by only 1 mv compared to the ordinate for a potassium concentration of 440 mM.

The above parameters should also be corrected for activity coefficients. The mean activity coefficient of 0.5 M KCl is equal to 0.65 (Conway, 1952). If the concentration of the divalent cation is ignored, then the actual value of G should be divided by the square root of 0.65. Using this corrected value of G increases the value of d_t to 11 A. Thus, A_t in our experiments gives a value of 120 A^2. Multiplying M by its activity coefficient in equation 11 would also increase our estimate of k. This estimate, however, is only within an order of magnitude.

Each of the parameters in equation 11 influences the curve of $V_{1/2}$ vs. ln M in a quite different manner (cf. Fig. 6). A change in the parameter B, which depends upon the reference point for the measurement of the voltage shift, merely shifts the curve up or down along the $V_{1/2}$ coordinate. A change in the parameter k, which depends upon the strength of the binding between divalent cations and negative fixed charge sites, shifts the curve left or right along the ln M axis. The parameter d_t, which is a measure of the fixed charge density, determines the amplitude of the curve.

The maximum slope of the $V_{1/2}$ vs. ln M curve is determined primarily by d_t, but is also influenced by k. When k is large, the sites become saturated at low concentrations of divalent cations (cf. equation 7), and the curve in Fig. 6 is shifted to the left. In this case, the slope is relatively independent of k, and maximum slope can be related directly to d_t, as shown in Fig. 7. In our experiments, k was rather small, and Fig. 7 is only roughly true. For example, d_t = 10 A corresponds to a maximum slope of 7.2 mv/e-fold change of M in Fig. 7, compared to a value of 9.2 from the more accurate equation 11.

The amplitude of the $V_{1/2}$ vs. ln M curve is completely independent of k and B. The asymptote for high divalent cation concentrations can be seen from equation 11 to be:

$$V_{1/2} = B. \tag{12}$$

The asymptote for low divalent cation concentrations can be obtained by using a simplified version of equation 1 valid for uni-univalent ions:

$$\sigma = -\frac{2}{G} C^{1/2} \sinh \frac{H}{2} V. \tag{13}$$

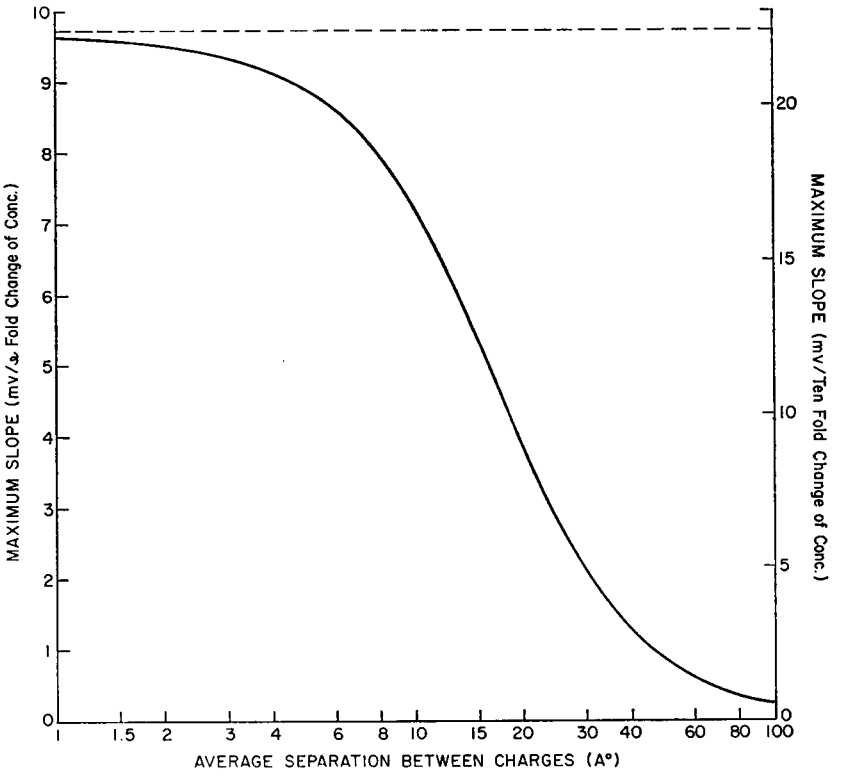

FIGURE 7 Relation between average charge separation and maximum rate of change of voltage shift for large values of equilibrium constant k.

This equation is valid for our experimental conditions at low divalent cation concentrations, since 0.5 M potassium chloride was present. Combining equations 3, 6, 10, and 13 results in:

$$d_i^2[kMe^{-2H(V_{1/2}-B)} + 1] = \frac{-G}{2C^{1/2}\sinh\frac{H}{2}(V_{1/2} - B)}. \quad (14)$$

The asymptote for low divalent cation concentration occurs when $M = 0$ in equation 14 and is:

$$V_{1/2} = B - \frac{2}{H}\sinh^{-1}\frac{G}{2C^{1/2}d_i^2}. \quad (15)$$

The amplitude of the $V_{1/2}$ vs. ln M curve is the difference between the values of $V_{1/2}$ in equations 12 and 15:

$$\text{Amplitude} = \frac{2}{H}\sinh^{-1}\frac{G}{2C^{1/2}d_i^2} \quad (16)$$

Amplitude vs. d_t from equation 16 is plotted in Fig. 8. The amplitude corresponding to d_t = 10 A is 68 mv. Even if our curve-fitting is inaccurate, however, the amplitude is at least 38 mv (cf. Fig. 6 and Table II). From Fig. 8, this gives a maximum value for d_t of 15 A. After correction for activity coefficients, this gives a lower limit for fixed charge density of one electronic charge/280 square A.

In our calculations, we have assumed that the negative fixed charge is uniformly distributed. Cole (1969) has shown that if the charge distribution is discrete rather than uniform, then more charge is required to produce a given potential. This effect increases our calculated charge density by a factor that may be as great as 2.5, depending upon the particular geometry of the charges with respect to the current flow.

Another assumption, which we have made, is that the negative fixed charge sites are either divalent or at least occur in closely spaced pairs. However, if the negative fixed charge sites are univalent, then it is possible that a sufficiently large concentration of divalent cation could result in a net positive charge on the membrane surface that is as great in magnitude as the original net negative charge. In this event, the voltage difference between asymptotes in Fig. 6 would correspond to a change in surface charge density of twice our maximum surface charge density rather than just the maximum surface charge density. Thus, this effect would possibly decrease our calculated charge density by a factor of two.

Since the nonhomogeneity of the sites and the possibility of univalent sites have

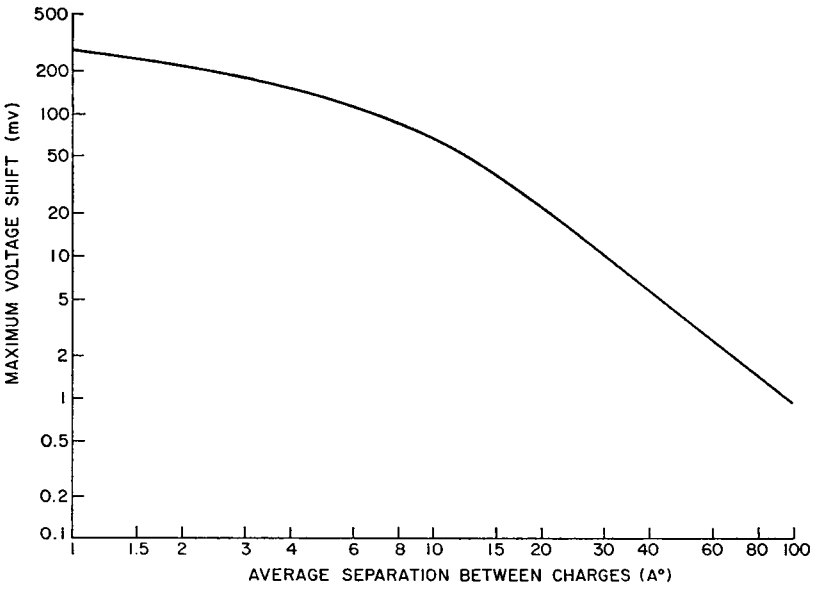

FIGURE 8 Relation between average charge separation and maximum voltage shift. Relationship calculated from equation 16. The value of C was set equal to 0.5 M.

opposite effects on our estimation of the charge density, it would appear that the value of one electron charge/120 square A is our best estimate for the external negative surface charge density.

Comparison With Other Charge Density Measurements

Our data indicate a maximum slope of about 9 mv/*e*-fold change of divalent cation concentration. Previously, Frankenhaeuser and Hodgkin (1957) obtained a slope of 6–9 mv/*e*-fold change of calcium for squid axons in solutions containing 10 mM potassium. These investigators also found a similar shift in the sodium conductance. Therefore, if the negative fixed charge model is correct, it is likely that the charge density of one charge/120 square A applies to the sodium channels as well as to the potassium channels.

Calcium also produces a similar voltage shift on myelinated nerve (Albrecht-Bühler, 1968; Frankenhaeuser, 1957; Hille, 1968), lobster axon (Julian et al., 1962), cockroach nerve (Narahashi, 1966), and muscle (Frankenhaeuser and Lännergren, 1967; Hagiwara and Takahashi, 1967).

Dan (1947) found that changes in calcium concentration shifted the zeta potential in eggs of the sea urchin, *Strongylocentrotus pulcherrimus*. On a semilog plot similar to our Fig. 6, the shifts were linear for relatively high concentrations of calcium, but departed from linearity for low calcium in a manner qualitatively similar to our results. Thus, Dan's electrokinetic results may also be explained by this negative fixed charge model.

Several other cations have also been shown to produce similar voltage shifts (Blaustein and Goldman, 1968), presumably by the same mechanism.

It is also possible to determine the charge density by varying the ionic strength with no divalent cations (cf. equation 13). This technique was used by Chandler et al. (1965) to determine the charge density at the internal side of the squid axon membrane near the sodium channel. They found a charge density of about one electronic charge/700 square A. Using a rather indirect method, Rojas and Atwater (1968) estimated the charge density at the internal side of the squid axon near the potassium channel to be about one electronic charge/1600 square A.

It would be interesting to compare these values of surface charge density near the ionic channels with the average charge density for the entire axonal membrane. But such a value is not available. The charge densities for other membranes, as measured by electrophoresis, appear to be smaller. Elul (1967) has found that the surface charge density on the membrane of cells of a variety of types, including cerebellar neurons and erythrocytes, is nearly the same, but could not measure the value directly. The value for erythrocytes, however, had been previously measured (Abramson et al., 1964), and is about one electronic charge/2000 square A. Recently, Segal (1968) has used electrophoresis to measure the surface charge density at the shear surface of squid and lobster axons. Since there are closely held layers

of Schwann cell and connective tissue surrounding these axons, it is quite possible that his measurement applies to these surrounding cells rather than to the axonal membranes. In any event, he found a charge density for squid axons of one electronic charge per 80,000 square A.

There are no inconsistencies in the measurements mentioned above. In the region around the conducting channels, the surface charge density appears to be somewhat greater on the outside than on the inside, but it is not yet possible to compare these values with the average surface charge density over the entire axonal membrane.

The authors acknowledge the helpful criticism from members and associates of the Laboratory of Biophysics, NINDS, NIH and in particular Dr. Kenneth S. Cole and Dr. L. Goldman. We also acknowledge the great help of John Shaw by aiding us in use of the the computer.

Received for publication 19 August 1968.

REFERENCES

ABRAMSON, H. A., L. S. MOYER, and M. H. GORIN. 1964. Electrophoresis of Proteins. Hafner Publishing Co., Inc., New York.
ALBRECHT-BÜHLER, G. 1968. *Pflügers Archiv.* **300**:23.
BLAUSTEIN, M. P., and D. E. GOLDMAN. 1968. *J. Gen. Physiol.* **51**:279.
CHANDLER, W. K., A. L. HODGKIN, and H. MEVES. 1965. *J. Physiol.* **180**:821.
COLE, K. S. 1969. *Biophys. J.* **9**:465.
COLE, K. S., and J. W. MOORE. 1960. *J. Gen. Physiol.* **5**:971.
CONWAY, B. E. 1952. Electrochemical Data. Elsevier Publishing Co., New York.
CURTIS, H. J., and K. S. COLE. 1942. *J. Cell. Comp. Physiol.* **19**:135.
DAN, K. 1947. *Biol. Bull.* **93**:267.
EHRENSTEIN, G., and D. L. GILBERT. 1966. *Biophys. J.* **6**:553.
EHRENSTEIN, G., and D. L. GILBERT. 1968. *Biophys. J.* **8**:A132.
ELUL, R. 1967. *J. Physiol.* **189**:351.
FRANKENHAEUSER, B. 1957. *J. Physiol.* **137**:245.
FRANKENHAEUSER, B., and A. L. HODGKIN. 1957. *J. Physiol.* **137**:218.
FRANKENHAEUSER, B., and J. LÄNNERGREN. 1967. *Acta Physiol. Scand.* **69**:242.
GILBERT, D. L., and G. EHRENSTEIN. 1965. Abstracts of the 23rd International Congress of Physiological Sciences. Tokyo, Japan. 86.
GOLDMAN, L. 1968. *J. Cell. Physiol.* **71**:33.
GOODFORD, P. J. 1966. *J. Physiol.* **186**:11.
GRAHAME, D. C. 1947. *Chem. Rev.* **41**:441.
HAGIWARA, S., and K. TAKAHASHI. 1967. *J. Gen. Physiol.* **50**:583.
HILLE, B. 1968. *J. Gen. Physiol.* **51**:221.
HODGKIN, A. L. 1958. *Proc. Roy. Soc. B* **148**:1.
JULIAN, F. J., J. W. MOORE, and D. E. GOLDMAN. 1962. *J. Gen. Physiol.* **45**:1217.
LECAR, H., G. EHRENSTEIN, L. BINSTOCK, and R. E. TAYLOR. 1967. *J. Gen. Physiol.* **50**:1499.
MANERY, J. 1966. *Fed. Proc.* **25**:1804.
NARAHASHI, T. 1966. *Comp. Biochem. Physiol.* **19**:759.
ROJAS, E., and I. ATWATER. 1968. *J. Gen. Physiol.* **51**:131S.
SCHMID, R. W., and C. N. REILLEY. 1957. *Anal. Chem.* **29**:264.
SEGAL, J. R. 1968. *Biophys. J.* **8**:470.
TASAKI, I., T. TEORELL, and C. S. SPYROPOULOS. 1961. *Am. J. Physiol.* **200**:11.